Citation: Molecular Therapy—Nucleic Acids (2016) 5, e302; doi:10.1038/mtna.2016.18
Official journal of the American Society of Gene & Cell Therapy

www.nature.com/mtna

METHODS: ORIGINAL ARTICLE

A Biofunctional Molecular Beacon for Detecting Single Base Mutations in Cancer Cells

Haiyan Dong[1,2], Ji Ma[1], Jie Wang[1], Zai-Sheng Wu[1], Patrick J Sinko[2] and Lee Jia[1]

The development of a convenient and sensitive biosensing system to detect specific DNA sequences is an important issue in the field of genetic disease therapy. As a classic DNA detection technique, molecular beacon (MB) is often used in the biosensing system. However, it has intrinsic drawbacks, including high assay cost, complicated chemical modification, and operational complexity. In this study, we developed a simple and cost-effective label-free multifunctional MB (LMMB) by integrating elements of polymerization primer, template, target recognition, and G-quadruplex into one entity to detect target DNA. The core technique was accomplished by introducing a G-hairpin that features fragments of both G-quadruplex and target DNA recognition in the G-hairpin stem. Hybridization between LMMB and target DNA triggered conformational change between the G-hairpin and the common C-hairpin, resulting in significant SYBR-green signal amplification. The hybridization continues to the isothermal circular strand-displacement polymerization and accumulation of the double-stranded fragments, causing the uninterrupted extension of the LMMB without a need of chemical modification and other assistant DNA sequences. The novel and programmable LMMB could detect target DNA with sensitivity at 250 pmol/l with a linear range from 2 to 100 nmol/l and the relative standard deviation of 7.98%. The LMMB could sense a single base mutation from the normal DNA, and polymerase chain reaction (PCR) amplicons of the mutant-type cell line from the wild-type one. The total time required for preparation and assaying was only 25 minutes. Apparently, the LMMB shows great potential for detecting DNA and its mutations in biosamples, and therefore it opens up a new prospect for genetic disease therapy.
Molecular Therapy—Nucleic Acids (2016) **5**, e302; doi:10.1038/mtna.2016.18; published online 5 April 2016

Introduction

Convenient, sensitive, and selective detection of nucleic acid sequences and other biomarkers has become increasingly important in gene profiling, drug screening, food safety, environmental analysis, forensic identification, and especially in human disease diagnosis.[1–7] Among these diseases, cancer so far remains one of the leading killers of human beings. Many efforts have been made toward early theranostics for carcinogenesis, cancer metastasis, and prognosis. As a typical cancer biomarker and its direct connection with transcriptional regulation and biological functions of some proteins,[8] mutant *p53* gene provides valuable information for early cancer diagnosis. Rapid genotyping methods for detecting *p53* gene and mutations are benefits for human health, and them particularly could help early diagnosis of cancer development and consequently increase the success of the treatment. As a result, *p53* gene is often used as the target model for developing highly sensitive methods of detecting nucleic acid mutations which are of great value.

In the past, many analytical methods have been developed for detection of both normal DNA and mutant DNA, especially by using the modern fluorescence, electrochemistry, and chemiluminescence methodologies. In these methods, molecular beacons (MBs) have been widely applied owing to their inherent advantages such as high specificity, sensitivity, rapid hybridization, convenient signal measurement, and easy adjustment.[9–11] However, MBs still suffer from some inherent deficiencies in practical application. For instance, oligonucleotide probes must be labeled with different sequences and dyes during assay optimization, which increase development cost and are time-consuming. Although many efforts have been made to develop new MBs[12–17] to improve their quality, simplicity, sensitivity, and robustics of new generation of MBs, simplifying the probe synthesis and decreasing the assay cost are still challenging. The multifunctional olignucleotide probes without any chemical modification should be a promising technology for the target DNA detection.

Because signals generated by the hybridization of MBs from the nano-amount of target DNA are often difficult to be detected, various signal amplification technologies such as rolling circle amplification (RCA), polymerase chain reaction (PCR),[18] and isothermal circular strand-displacement polymerization (ICSDP) have been introduced into the MB-based

[1]Cancer Metastasis Alert and Prevention Center, and Pharmaceutical Photocatalysis of State Key Laboratory of Photocatalysis on Energy and Environment, College of Chemistry, Fujian Provincial Key Laboratory of Cancer Metastasis Chemoprevention and Chemotherapy, Fuzhou University, Fuzhou, China; [2]Ernest Mario School of Pharmacy, Rutgers, The State University of New Jersey, Piscataway, New Jersey, USA. Correspondence: Lee Jia, Cancer Metastasis Alert and Prevention Center, and Pharmaceutical Photocatalysis of State Key Laboratory of Photocatalysis on Energy and Environment, College of Chemistry, Fujian Provincial Key Laboratory of Cancer Metastasis Chemoprevention and Chemotherapy, Fuzhou University, 523 Industry Road, Science Building, 3FL. Fuzhou, Fujian 350002, China. E-mail: pharmlink@gmail.com; cmapcjia1234@163.com or Zai-Sheng Wu, Cancer Metastasis Alert and Prevention Center, and Pharmaceutical Photocatalysis of State Key Laboratory of Photocatalysis on Energy and Environment, College of Chemistry, Fujian Provincial Key Laboratory of Cancer Metastasis Chemoprevention and Chemotherapy, Fuzhou University, 523 Industry Road, Science Building, 3FL. Fuzhou, Fujian 350002, China. E-mail: wuzaisheng@163.com
Keywords: DNA mutation; label-free multifunctional molecular beacon; *p53* gene; therapy
Received 4 December 2015; accepted 9 February 2016; published online 5 April 2016. doi:10.1038/mtna.2016.18

sensing systems. In a typical RCA process, the enzyme with strand displacement ability is used to amplify the target signals by extending a primer over a circular single-stranded DNA as the template and producing a long single-stranded sequence with repeat units. However, due to the lack of useful reporting dyes that match precisely the signal polymerization products and single-stranded DNA sequences, RCA technique is practically difficult to be used in a label-free sensing system if the required DNA is unavailable for the RCA technique. PCR, as a typical amplification protocol, has been widely used to detect target DNA via yielding doubled-stranded DNA sequences in the amount enough to be shown by the label-free fluorescent signal generated from intercalation dye SYBR Green I.[19] However, PCR suffers the drawbacks of easy contamination, high assay cost, rigorous temperature cycles, and complicated operation.[20,21] Recently, the emerging technique, *i.e.*, ICSDP,[22–24] has being applied to the MB-based sensing systems to detect target DNAs.[25–29] In these sensing systems, nucleic acid strands are circularly displaced during the polymerization reaction, and therefore the target hybridization, polymerization, and displacement can be repeatedly cycled until the signal amplification is achieved high enough. ICSDP does not need the specific recognition site, and it can be conveniently utilized to design different biosensors for sensitive DNA detection.[30–33] Combination of ICSDP with intercalating SYBR Green I makes it possible for development of a label-free MB-based system for DNA detection. However, this-type of biosensors needs various species (polymerization primer, template, and target recognition) to collaboratively work together to amplify the signals. Thus, it is very necessary to design a multifunctional label-free MB that could integrate the aforementioned elements into a single entity to detect DNA mutations in a programmable and seamless manner.

Based on our previous experiences at developing a primer-integrated MB for detecting tumor suppressor,[34] in the present study, we further developed a primer-integrated label-free multifunctional molecular beacon (LMMB) for sensitive detection of target DNA via integrating the target recognition sequence, polymerization primer, template, and G-quadruplex structure into a single entity. The LMMB is suitable for the ICSDP amplification of target DNA without any additional oligonucleotide probe. The polymerization products were designed to contain the double-stranded fragments available for the intercalation of SYBR Green I to signal the hybridization event. The model target DNA can force the LMMB to change its molecular configuration from large common hairpin to a small G-quadruplex-contained hairpin to trigger an isothermal circular polymerization reaction. Besides excellent advantages, such as simplicity, low cost, and high sensitivity, this integrative probe is suitable for quantifying trace amount of the target DNA, and even for identifying a single base mutation. The design and working principle of the proposed LMMB are reported below.

Results and discussion

LMMB design and principle of target DNA-triggering signal amplification

According to the scientific literatures,[25,35,36] the ICSDP-based biosensor usually needs a primer sequence in addition to a signaling probe. This template/primer, although without the need of polymerization, often produces high nonspecific noise. This often could generate false-positive signals especially in a label-free system. Additionally, this biosensor requires a complicated operation, suffers from low selectivity and high cost. Even though some new strategies, which separate polymerase from template until the reaction temperature was reached,[27] and conformational transition was made between hairpin structures,[37] have been explored during the development of ICSDP amplification to decrease the nonspecific noises, no substantial progress has been achieved. The design of a cost-effective probe with high sensitivity and robotic reproducibility remains very challenging. To overcome the technical problem, we developed the LMMB via introducing G-rich fragment into MB probe. The LMMB sequence was shown in **Table 1**. The LMMB contained 73 bases. In the middle of the loop was 32 bases that possessed the recognition sequence complementary to the target *p53* gene. Two complementary 17-base fragments were made, including a G-rich fragment that could be hybridized to each other to form a long stem of 17 bases, and a single-stranded 7-base overhang at the 3' terminus. Comparing with the traditional MB,[38] in which G-rich fragment is often involved in the LMMB, we introduced the G-rich fragment into the stem of loop. This unique structural design made it easy for the conformational change between the large common C-hairpin and small G-rich hairpin. As a result, significant signal amplification in detecting target DNA could be obtained.

We also integrated the LMMB with target DNA recognition, polymerization primer, and template into one entity. The polymerized double-stranded (ds) DNAs could be monitored with the aid of intercalation dye, making the ICSDP amplification effective. **Figure 1** elucidated the working principle of LMMB. In the absence of target *p53* gene, LMMB self-assembled into the C-hairpin similar to the stem-loop configuration of a typical MB. In this case, no high fluorescence peak could be detected even in the presence of the intercalation dye due to a relatively short double-stranded DNA sequence and the fluorescence quenching effect by G-rich fragments.[39–42]

In contrast, in the presence of target *p53* gene without the polymerase, the target DNA hybridization could generate not only long double-stranded DNA fragment, but also force C-hairpin stem to open and facilitate the formation of G-quadruplex-contained hairpin (G-hairpin) structure. With the aid of the unique G-quadruplex noncanonical secondary structure, the target DNA/LMMB hybrids could be assembled into the octamer and loose dimer to a large quantity via the sticky-end pairing effect (see the **Supplementary Materials**), leading to the additional double-stranded DNA fragments. After intercalating SYBR Green I into double-stranded DNA portions, the fluorescence signal could be detected in comparison with the negative control. When the polymerase and dNTPs were added to this sensing system, self-polymerization of the target DNA-hybridized LMMBs from its 3' terminus occurred automatically without any additional template and primer. The reaction displaced the target DNA, generated longer double-stranded DNA fragments, and resulted in the enhanced fluorescence signal. Moreover, the extended LMMBs might assemble into the tight dimers that shifted the dynamic equilibrium between G-hairpin, octamer, and loose dimer toward the polymerization. Meanwhile, the displaced target DNA hybridized to

Table 1 Sequence of oligonucleotides designed in this study

Name	Sequence (5′ to 3′) description[a]
Probe1 (P1, LMMB)	5′-**CCCAACCCGCCCTACCC**CACAAACACGCACCTCAAAGCGCTGAGGCTTT**GGGTAGGGCGGGTTGGG**TTTGCCT-3’
Probe2 (P2)	5′-**AACCCGCCCTACCC**CACAAACACGCACCTCAAAGCGCTGAGGCTTT**GGGTAGGGCGGGTT**GGGTTTGCCT-3′
Probe3 (P3)	5′-**CCGCCCTACCC**CACAAACACGCACCTCAAAGCGCTGAGGCTTT**GGGTAGGGCGG**GTTGGGTTTGCCT-3′
Probe4 (P4)	5′-**CCCTACCC**CACAAACACGCACCTCAAAGCGCTGAGGCTTT**GGGTAGGG**CGGGTTGGGTTTGCCT-3′
Probe5 (P5)	5′-**TACCC**CACAAACACGCACCTCAAAGCGCTGAGGCTTT**GGGTA**GGGCGGGTTGGGTTTGCCT-3′
Target DNA (p53 gene)	5′-GGAACAGCTTTGAGGTGCGTGTTTGTGCCTG-3′
Mutant target DNA1 (M1)	5′-GGAACAGCTTTGAGGTGCaTGTTTGTGCCTG-3′
Mutant target DNA2 (M2)	5′-GGAACAGCTTTGAGGTGCaTGTTTtTGCCTG-3′
Mutant target DNA3 (M3)	5′-GGAACAGCTTTGAGtTGCaTGTTTtTGCCTG-3′
Mutant target DNA4 (M4)	5′-GGAACAtCTTTtAGGTGCaTGTTTtTGCCTG-3′
Mutant target DNA5 (M5)	5′-GGAACAGCTTTGAGGTGCGTGTTTtTGCCTG-3′
Target DNA 1 (T1)	5′-TTTGAGGTGCGTGTTTGTGCCTG-3′
Mutant DNA1 (MT1)	5′-TTTGAGGTGCaTGTTTGTGCCTG-3′
Target DNA 2 (T2)	5′-GAGGTGCGTGTTTGTGCCTG-3′
Mutant DNA2 (MT2)	5′-GAGGTGCaTGTTTGTGCCTG-3′
Target DNA 3 (T3)	5′-GGTGCGTGTTTGTGCCTG-3′
Mutant DNA3 (MT3)	5′-GGTGCaTGTTTGTGCCTG-3′
Target DNA 4 (T4)	5′-GTGCGTGTTTGTGCCTG-3′
Mutant DNA4 (MT4)	5′-GTGCaTGTTTGTGCCTG-3′
Phosphorylated replication product DNA (PRPD)	5′-p-CAGCGCTTTGAGGTGCGTGTTTGTGGGGTAGGGCGGGTTGGG-3′
non-complementary DNA (NCD)	5′-GTCTAGAAATCTAACCGTACAGTATTTTCC-3′
Forward primer	5′-TGGTAATCTACTGGGACGGA-3′
Reverse primer	5′-CGCCGGTCTCTCCCAGGACA-3′

[a]In the LMMB, the bold base fragments were complementary to each other and formed the stem. The sequence with gray background hybridized with target p53 DNA. The short underlined fragments denote the complementary sequences that form G-quadruplex structure in the middle of the LMMB. The LMMB was designed to contain 73 bases, while probe2, probe3, probe4, and probe5 were shortened by 3 bases, 6 bases, 9 bases, and 12 bases at the 5’ terminal, respectively. The complementary base length of target DNA1 to 4 was gradually decreased to match the length of the target p53 gene. The boxed bases in lowercase in mutant DNAs indicated the mutant points. The 5′ end of replication product DNA (PRPD) was phosphorylated, and its sequence was designed to match with the bold portion of LMMB just as its name implied. Additionally, noncomplementary DNA was designed to contain 30 bases, and the Forward primer and Reverse primer were designed to contain 20 bases for PCR amplification of tumor cells.
LMMB, label-free multifunctional molecular beacon

another LMMB and induced the next cycle of the hybridization/polymerization/displacement reaction. The reaction cycle thus repeated (**Figure 1**). As a result, the tight dimers were significantly accumulated which substantially enhanced the fluorescence intensity of sensing system in the presence of signal indicator SYBR Green I. Moreover, the matching degree between target DNA and LMMB was designed to directly influence the amplification process. Thus, a very minute amount of target DNA in complicated samples could be sensitively and efficiently detected, and the point mutations could be reliably pinpointed by the novel LMMB.

Clearly, during the cyclic amplification, only one LMMB was needed and it served for the target recognition element, polymerization primer and template all together. Moreover, double-stranded hybrid generated from the extension of LMMB was ready for intercalation of SYBR Green I necessary for generation of fluorescence signal without any additional treatment. This label-free multifunctional MB represents an efficient and sensitive method compared with the conventional MB, in which the target cannot trigger cyclic polymerization without the nicking enzyme.[43]

Exploration of LMMB sequence

It seems a great challenge to integrate different functional nucleotides or nucleic acids into one probe to sensitively and efficiently detect target DNA without any exogenous auxiliary oligonucleotide. In the present LMMB, the G-quadruplex mediated a change in configuration between C-hairpin and G-hairpin. The G-rich fragment was designed as a unique functional nucleic acid that could readily fold into G-quadruplex structure without a change in the base length.[44] To achieve a desirable assay capacity, we optimized the thermal stability of C-hairpin via regulating the stem base length. We found that when the stem was very short, some LMMBs might open even in the absence of target DNA and the subsequent amplification reaction occurred and generated the high fluorescence background. Conversely, a very long stem could make the LMMB too stable to screen the target DNA hybridization. Thus, the reasonable sequence design of LMMB was of vital importance, and it should be firstly explored. To optimize the probe sequence to sensitively detect target DNA, we synthesized different probes and evaluated their sensitivity for detecting the target DNA under the same conditions. The experimental results were shown in **Figure 2**. As demonstrated in **Figure 2a**, the data indicated that target DNA hybridization unambiguously induced individual fluorescence responses, resulting in different optical signals and background intensities. To accurately evaluate the sensing ability of each probe, we calculated the fluorescence peak ratio as shown in **Figure 2b**. There was no substantial change in signal intensity between P1, P2 and P3, while a remarkably low signal was observed for the P4 and P5. The decrease in signal intensity should be attributed to the increase in the fluorescence background. The data demonstrated that the length of a stem is an essential element for

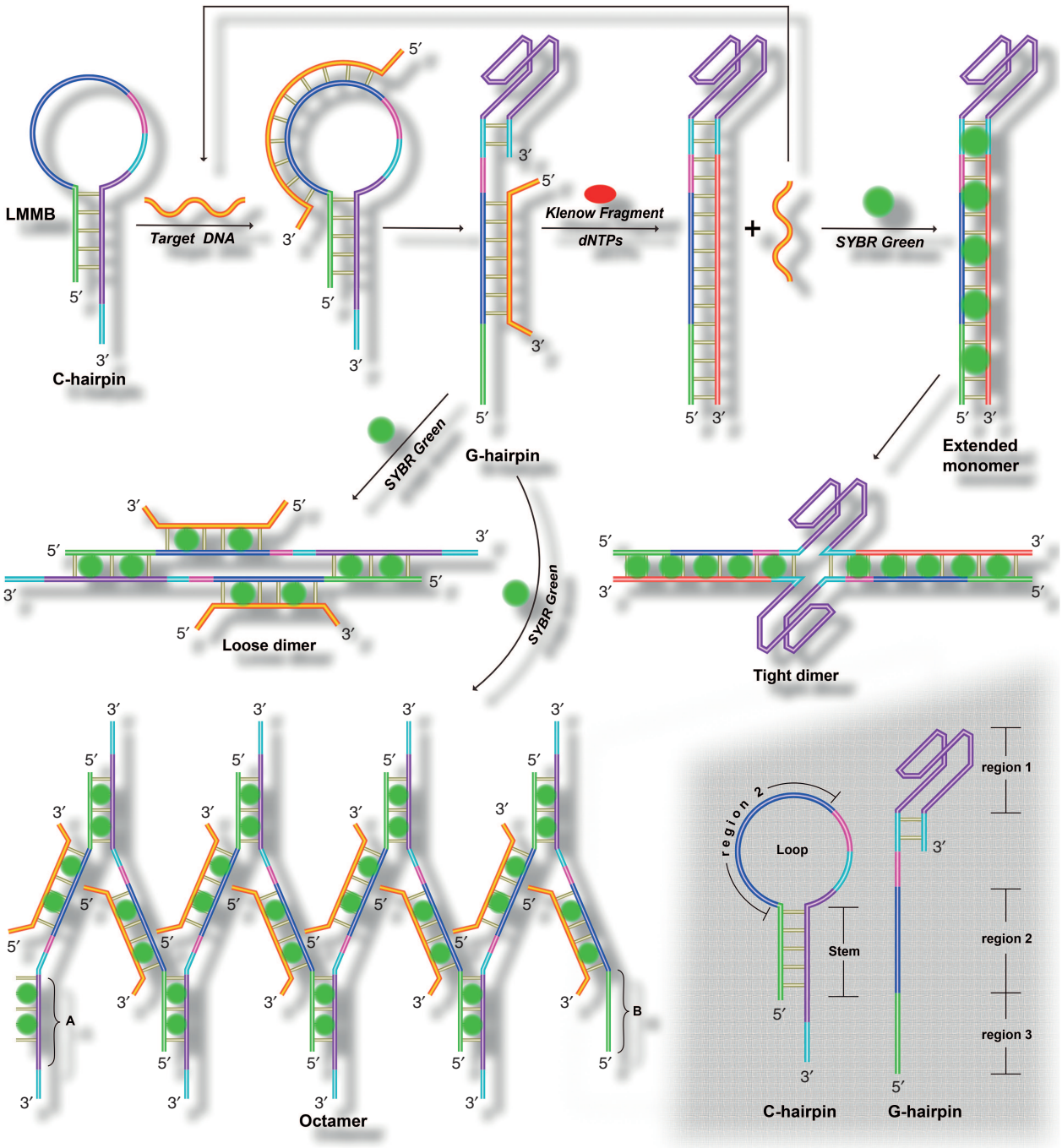

Figure 1 Schematic illustration of proposed LMMB for *p53* gene detection. The fragments "A" and "B" in octamer are capable of hybridizing with each other. The functional fragments of LMMB are illustrated in the lower right panel: C-hairpin, a hairpin structure with a common loop; G-hairpin, a hairpin structure with a G-rich loop; Region 1, G-quardruplex; Region 2: recognition sequence of *p53* gene; Region 3: the base fragment partially complementary to Region 1. The details of the molecular mechanismscan be read in the text.

the efficacy of the multifunctional probe. We selected P1 as the optimized LMMB in the following experiments.

Feasibility of LMMB-based signal amplification for *p53* detection

To verify the feasibility of the designed LMMB for the target DNA detection, we detected the target *p53* gene in the presence of various components. As shown in **Figure 3a**, no obvious change in fluorescence peak was detected when *p53* DNA was absent no matter if the noncomplementary MB and/ or polymerase were present (line a, line b, and line c). The results indicated that the designed LMMB with the C-hairpin structure was stable enough to the KF polymerase. In the presence of target *p53* gene, the fluorescence intensity of the sensing system in the absence of KF polymerase increased from 45 (line b, in the absence of target) to 184 au (line d), suggesting that

more SYBR Green I was intercalated into the double-stranded segment, and the hybridization between *p53* gene and LMMB was formed. Interestingly, in the presence of KF polymerase and dNTPs, target DNA hybridization caused a significant fluorescence increase (line e, 513 au) compared with the blank (line c, 50 au), suggesting the success of converting the target DNA/probe hybridization into the enhanced fluorescent signal. **Figure 3a** showed strong evidence that the newly-proposed label-free multifunctional molecular beacon could be used to implement the signal amplification of *p53* target DNA.

To verify the utility of the proposed LMMB, we performed the native-PAGE gel electrophoresis analyses, and the results were shown in **Figure 3b**. The molecular weight and configuration of DNAs were reflected by the electrophoresis images, suggesting the formation of amplification products and the relevant specimens. Lane a exhibited only one clear band higher than 50 bps (base pairs) (lane M, markers), corresponding to the LMMB (73 bases) with a large hairpin (C-hairpin, see **Supplementary Figure S3**) structure. As shown in lane b, without polymerase, the hybridization of LMMB to target *p53* gene induced the appearance of two new bands, dim band (near 100 bps, base pairs) with a slow mobility and bright band (near 400 bps, base pairs) with much slower mobility, while, the band of LMMB disappeared. The dim band should be loose dimers (208 bases) and the bright band should be Octamers (see **Supplementary Figure S5,** 8×104 bases) of *p53*/LMMB hybrid that was about eightfold higher than the monomer of *p53*/LMMB hybrid (G-hairpin, see **Supplementary Figure S4,** 104 bases), and Octamers were the main products. This result indicated the sufficient hybridization between LMMB and target DNA. The

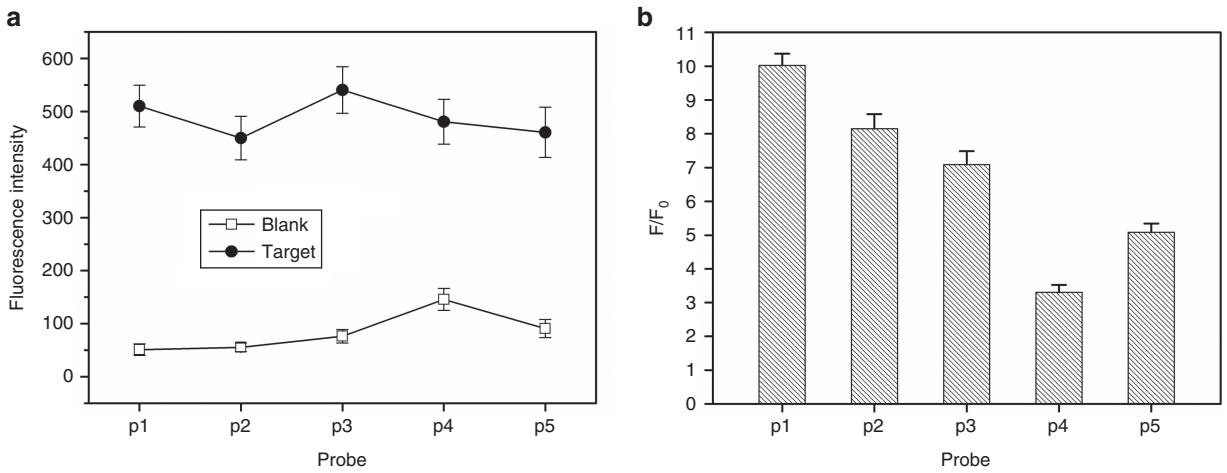

Figure 2 The optimization of label-free multifunctional molecular beacons (LMMBs). (**a**) The fluorescence intensities of LMMBs that contained different probes (P1-P5) in the presence and absence of target DNA; (**b**) The signal-to-background ratio (F/F_0) of corresponding samples, where F and F_0 are the fluorescence intensity at 524 nm in the presence and the absence of target *p53*, respectively. The concentrations of species: [LMMB] = 0.4 μmol/l, [*p53* DNA] = 0.2 μmol/l, [KF] = 2.5 U and [dNTPs] = 0.2 mmol/l. The polymerization time was adopted to 20 minutes. Error bars indicate standard deviation of measurements ($n = 3$).

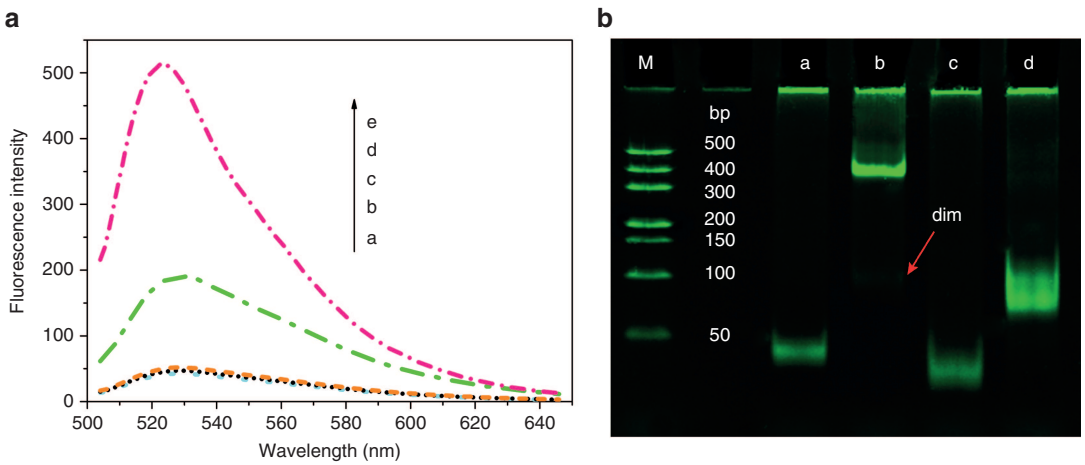

Figure 3 Feasibility of the designed label-free multifunctional molecular beacon (LMMB) for *p53* gene detection. (**a**) Fluorescence emission spectra of the sensing system containing (**a**) LMMB + NCD, (**b**) LMMB, (**c**) LMMB + dNTPs + polymerase, (**d**) LMMB + *p53* DNA, (**e**) LMMB + *p53* DNA + dNTPs + KF polymerase. (**b**) Native-PAGE (10%) gel electrophoretic analysis of the identical samples: (**a**) LMMB, (**b**) LMMB + *p53* DNA, (**c**) LMMB + dNTPs + polymerase, (d) LMMB + *p53* DNA + dNTPs + KF polymerase. The concentrations of species: [LMMB]= 0.4 μmol/l; [*p53* DNA] = 0.2 μm; [NCD] = 0.2 μmol/l; [KF] = 2.5 U; [dNTPs] = 0.2 mmol/l. The polymerization was performed at 37 °C for 20 minutes.

hybrid may self-assemble into the advance DNA structures with higher molecular weight (contributing to the gel mobility shift in the bright band of lane b in **Figure 3b**), and expectedly obvious fluorescence peak is detected (line d of **Figure 3a**). In lane d of **Figure 3b**, with KF polymerase, only one bright and large band was observed and the DNAs in this band presented a faster and dramatically brighter gel mobility than dim band and bright band in lane b, indicating a lower molecular weight. Meanwhile, a dramatic fluorescence increase was observed in line e of **Figure 3a**, suggesting a unique molecular structure different from the dim band and bright band in lane b. Presumably, DNA complexes in band d should be the tight dimers (see **Supplementary Figure S6**) of the extended LMMB (230 bases), but mobility of this band was faster than marker of 100 bp (base pairs) because there were two intramolecular G-quadruplex structures that made the tight dimer shrink and decreased the steric hindrance (the detail structures was shown in **Figure 1** and more supporting data was presented in **Figure 4**. Lane c represented nearly the same brightness and slightly higher gel mobility compared with the LMMB band (lane a), suggesting that the polymerization reaction of the probe did not occur in the presence of polymerase, and the gel mobility of LMMB was slightly changed by the polymerase.

Evidently, the data strongly suggested that amplification detection of target *p53* gene may be accomplished by the LMMB probe and the expected fluorescence signal should be attributed to the significant molecular configuration change of LMMB triggered by target DNA. The observations were in accordance with the fluorescence spectra and the molecular mechanism of LMMB which resulted in evidence of transducing the biorecognition into a sensitive signal.

Gel electrophoresis analysis of tight dimer

As indicated in **Figure 1**, three possible DNA conformational structures (loose dimer, octamer and tight dimer) were possibly formed in this system. To verify the tight dimer, we designed an oligonucleotide (called PRPD, **Table 1**) that contained the same base sequence as the extended part of LMMB, and carried out the comparative gel electrophoresis analyses. After hybridization of PRPD with LMMB, the ligation automatically took place to seal the nick. The gel electrophoresis image (**Figure 4**) showed that there was no obvious difference between lane a, b, and c, indicating that the target DNAs could not interact with the ligation products (introduced in lane c), and lane a contained the same DNA complexes as the lane b. Structurally, the assemblies should be the extended LMMB dimmers (namely the tight dimer) because their base number was close to the marker of 100 bp equaling to 200 bases, which the monomer and trimer had the base number 115 and 345, respectively). These images demonstrated the completion of the tight dimmers resulted from the target DNA-induced polymerization amplification.

Detection sensitivity of the LMMB

Under the optimal experimental conditions (see **Supplementary Figures S1 and S2**), we evaluated the sensitivity of the designed LMMB via detecting the different concentrations of target DNA ranging from 2.5×10^{-10} to 2.75×10^{-7} M. As shown in **Figure 5a**, the fluorescence response intensity increased with the increasing concentrations of the target

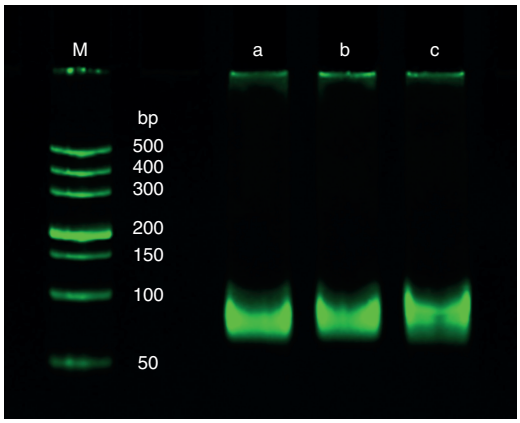

Figure 4 The electrophoresis-based verification of tight dimers resulted from the self-assembly of polymerization products in the label-free multifunctional molecular beacon (LMMB)-based system. (**M**) the molecular weight ladders, (**a**) LMMB + *p53* DNA + dNTPs + KF polymerase, (**b**) LMMB + PRPD + Ligase, (**c**) LMMB + PRPD + Ligase + *p53* DNA. The concentrations of species are as follows: [LMMB] = 0.4 μmol/l; [*p53* DNA] = 0.2 μmol/l; [PRPD] = 0.2 μmol/l; [KF] = 2.5 U; [dNTPs] = 0.2 mmol/l; [Ligase] = 2.5 U. Both polymerization and ligation were run for 20 minutes.

p53 DNA. The inset showed the fluorescence spectra at low concentrations of target *p53* DNA ranging from 2.5×10^{-10} to 2×10^{-9} M. The target *p53* DNA at concentration of 2.5×10^{-10} M could induce a detectable fluorescence change, and we defined the concentration as the limit of detection, which is lower than the usual limit of detection achieved by those typical MBs.[45] **Figure 5b** clearly showed a good dynamic relationship between the changes in fluorescence increase (ΔF) and the target *p53* gene concentration ranging from 2.0×10^{-9} to 1.0×10^{-7} M with R^2 value of the linear equation is 0.9902. The inset of **Figure 5a** showed the real fluorescent scan of the target DNA at low concentrations (0.25–1 nmol/l).

To validate the assay reproducibility, various concentrations of target *p53* DNA ranging from 5 to 10 nmol/l were repeatedly determined. As a result, the highest value of the relative standard deviations (RSD) 7.98% (n = 5) was achieved, suggesting that the method met our desired acceptance criteria of less than 10% RSD. The reproducibility data are seen in the **Supplementary Materials** (**Supplementary Table S1**).

Specificity of the LMMB in the absence and presence of noncomplementary DNA (NCD)

To evaluate the specificity of the LMMB-based sensing system, we designed two types of mutant target DNAs, the single-base or several-base mutation DNAs, and the noncomplementary DNA (NCD), and used the sensing system to distinguish one from another. The mutant DNAs could be divided into two groups (**Table 1**): in one group, each section (M1-M5) had the same base length; in another group, the base lengths decreased gradually from MT1 to MT4. All mutant DNAs had their own complementary counterparts as the controls. Moreover, M1, MT1, MT2, MT3, and MT4 each had one-base pair translocation from G to A (CGT to CAT) that might suppress *p53* activity in human cancers.[8] More than one base mutation in DNAs, M2, M3, and M4 (the

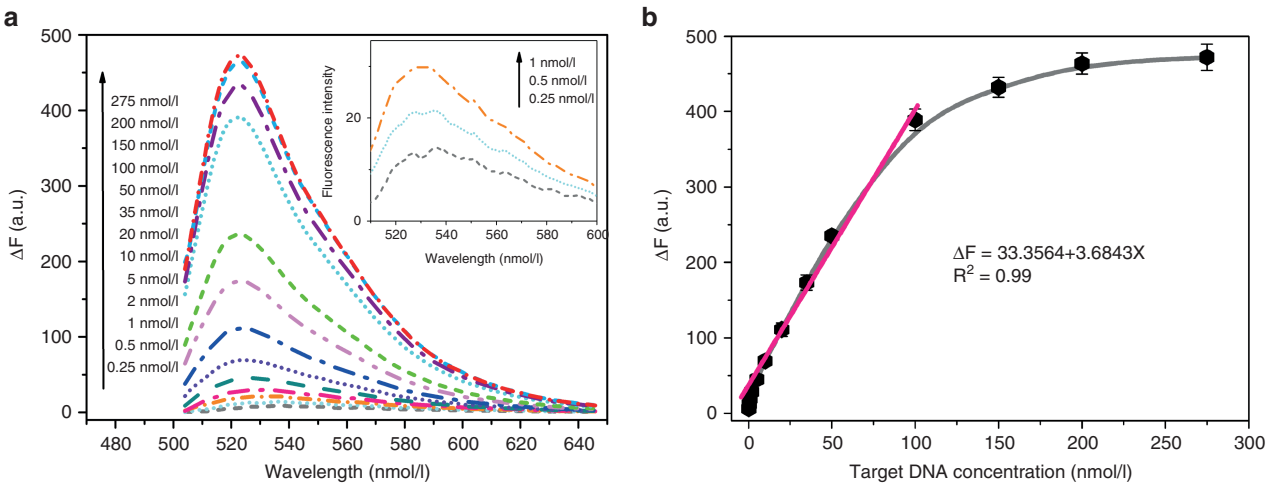

Figure 5 Dependence of fluorescence intensities on the target DNA concentrations. (**a**) Fluorescence spectra of label-free multifunctional molecular beacon (LMMB)-based sensing system in the presence of target DNA at the concentrations of 0.25, 0.5, 1, 2, 5, 10, 20, 35, 50, 100, 150, 200, and 275 nmol/l. The inset showed: the fluorescence spectra of low DNA concentrations ranging from 0.25 to 1 nmol/l, indicating the low limit of detection of the system; (**b**) Dynamic relationship of LMMB-based sensing system between the value of fluorescence increase $\Delta F(F\text{-}F_0)$ and target DNA concentrations, where F and F_0 are the fluorescence intensity at 524 nm in the presence and the absence of target *p53*, respectively. The ΔF denotes the value of fluorescence increased, and X represents target DNA concentrations; the error bars are standard deviations of measurements ($n = 3$) of each DNA concentration. The concentrations of species are [LMMB] = 0.4 μμ; [KF] = 2.5 U; [dNTPs] = 0.2 mmol/l. The polymerization time was 20 minutes.

fictitious mutation) were also designed to evaluate detection specificity of the LMMB.

The measured data of LMMB on the signals induced by M1-M5 in the absence of NCD were shown in **Figure 6a**,**b**. The fluorescence signals induced by M1 and M5 were 83 and 82%, respectively, based on the control target *p53* DNA fluorescence intensity. The result indicated that the LMMB could, sensitively enough, detect a single base mutation. The fluorescence intensities corresponding to M2, M3, and M4 were 68% ($P < 0.05$), 44%, and 46% ($P < 0.01$), respectively. **Figure 6b** showed the signals corresponding to other DNAs with the same single-base mutation but different base length. MT1 induced the fluorescence intensities of 81%. MT2, MT3, and MT4 induced the fluorescence intensities of 72% ($P < 0.05$), 68% ($P < 0.05$), and 42% ($P < 0.01$), respectively. The result suggested that decrease in the number of matched base pair between target DNA and sensing probe could further improve the LMMB capability of point mutation recognition.

To evaluate specificity of LMMB in more complex matrices, we measured the signals induced by M1-M5 in the presence of NCD. **Figure 6v** showed that the fluorescence signals induced by M1 and M5 were 86 and 80%, respectively. The signals corresponding to M2, M3, and M4 were 65% ($P < 0.05$), 46% and 50% ($P < 0.01$), respectively, similar to the results shown on **Figure 6a**. **Figure 6d** showed the signals triggered by other DNAs with the same single-base mutation but different base length. MT1, MT2, MT3 and MT4 induces the fluorescence intensities of 84%, 76% ($P < 0.05$), 65% ($P < 0.05$) and 46% ($P < 0.01$), similar to the results shown on **Figure 6b**. These data clearly indicated that the LMMB could specifically detect a signal base mutation occurred in the *p53* target DNA, even in the presence of many interfering noncomplementary DNA. The novel LMMB gained advantage over the previously reported MB[38] in terms of detection specificity.

Performance for analyzing real samples

PCR amplicons from cancer cell lines were used to further evaluate the practicality of this LMMB-based system. The corresponding PCR products from the human carcinoma cell line LOVO (the wild-type) and SW620 (the mutant-type) were analyzed in parallel using the LMMB. As shown in **Figure 7**, the fluorescent signal responding to the PCR-M with a signal point mutation was 79% ($P < 0.05$), suggesting that it is significantly lower than that obtained from the whole complementary target (PCR-T). If the hybridized fragment between target DNA and probe was shortened, the detection specificity could be further improved. Together, the result indicated that the present system has the potential for mutant DNA detection in real tumor samples.

Conclusions: significance and potentials of the LMMB

To simplify the probe design, we assembled several elements (polymerization primer, template G-quadruplex structure and target recognition sequence) into one probe, *i.e.*, the LMMB. This label-free probe was able to execute the ICSDP reaction for the amplified detection of DNA hybridization without any chemical modification, and only one-type of probe was needed for the sensing system. The detection of DNA biomarkers could be conducted without any nucleic acid sequence. During the configuration change of the LMMB, G-quadruplex structure plays a critical role in detecting nucleic acids. Besides the simplicity and convenience, this label-free multifunctional MB-based biosensor possesses other advantages as follows.

A labor-intensive study preparation and a complicated detection procedure are often required by the ICSDP

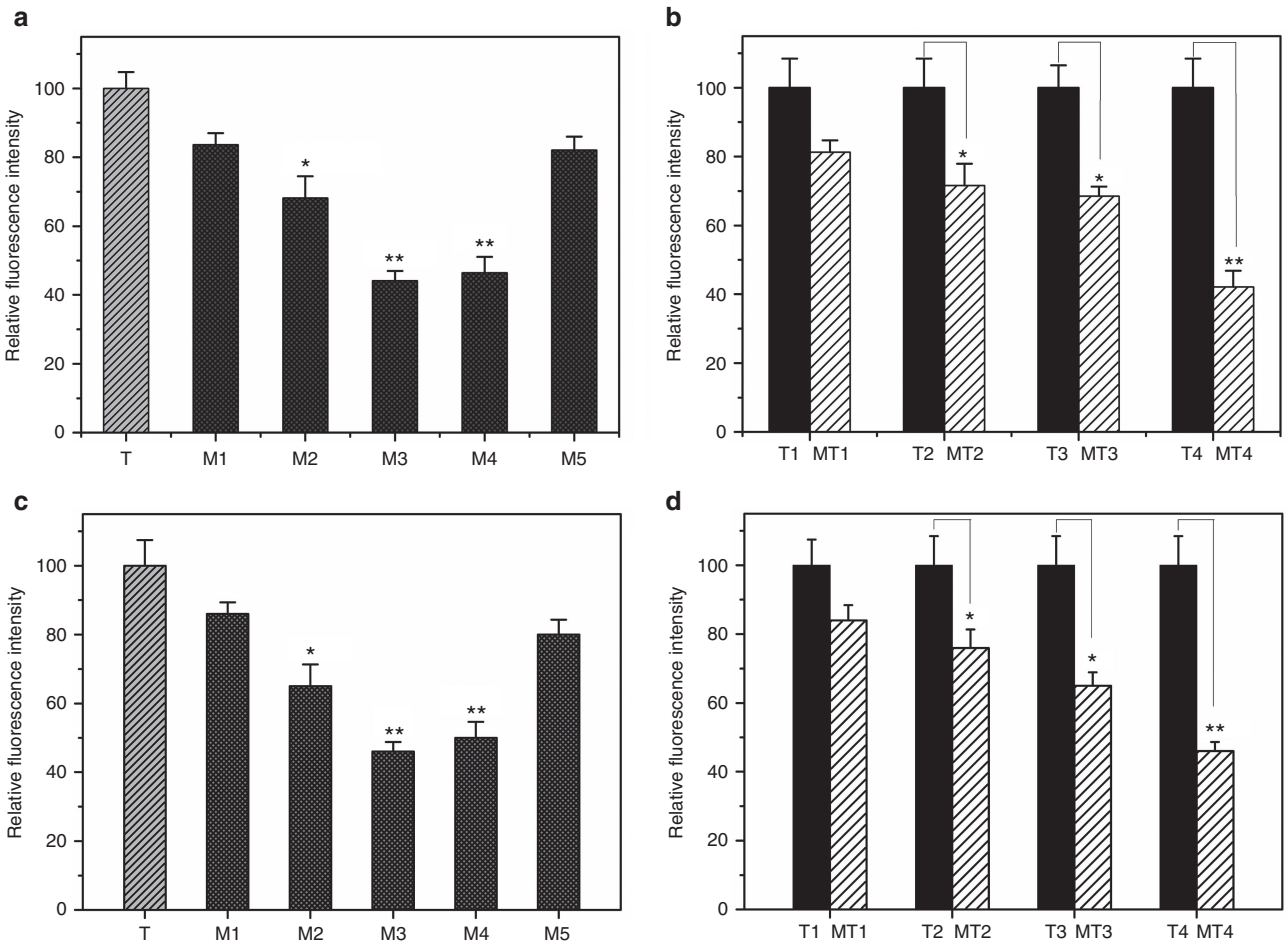

Figure 6 Comparative data on the detection specificity of label-free multifunctional molecular beacon (LMMB)-based sensing system in the presence and absence of noncomplementary DNA (NCD). (**a**) The relative fluorescence response (F_r) of LMMB-based sensing system induced by wild-type target DNA or mutant target DNAs (from M1 to M5) in the absence of NCD; (**b**) The relative fluorescence response (F_r) of LMMB-based sensing system induced by short target DNAs (from T1 to T4) and corresponding mutant target DNAs (from MT1 to MT4) in the absence of NCD; **c** and **d** are the same results obtained under the same conditions as **a** and **b** except that the NCD was presented. The F_r signal (%) was calculated by the equation: $F_r = (F_m - F_0)/(F_t - F_0) \times 100\%$, where F_t, F_m, and F_0 are the fluorescence intensities in the presence of target DNA, mutant target DNAs and blank, respectively. The signal intensity triggered by target DNA is defined as 100%. The concentrations of species: [NCD] = 0.2 μmol/l. Experiment conditions are same to those in **Figure 3**. Data shown are average values from three samples, form which the error bars were estimated. The statistical analysis represents the means ± SD of three independent measurements as compared with the control (*$P < 0.05$, **$P < 0.01$).

technique,[46,47] which usually takes a long time to run an analytical process. This limits the application of ICSDP technique in medical diagnosis and bioanalysis. The LMMB not only simplifies the detection procedure but also reduces the assay time. The total assay time required for preparation and enzyme inactivation is only 25 minutes, which is remarkably shorter than the time needed for the oligonucleotide probe-based assays.[48,49]

As indicated in the literature,[49] fluorescent probes are often used for generating a detectable signal, besides scission and/or ligation enzymes are utilized to convert the target/probe hybridization into more extension primers, and therefore the signal transduction process is mediated by several additional species. Contrarily, in the present LMMB system, the target/probe binding and primer extension by polymerase directly occur on the designed MB, and the target displacement can repeatedly proceed during the cyclical polymerization amplification to generate the double-stranded products that indicate the location of intercalation dyes. Thus, ligation and scission can be eliminated, and SYBR green I can be used to report the target DNA hybridization without additional chemically-modified oligonucleotide probes.

In short, we, for the first time, designed the LMMB by integrating all functional elements (polymerization primer, template, target recognition, and G-quadruplex structure) into one entity to execute the isothermal circular strand-displacement polymerization for signal amplification. The target DNA can induce the conformational change of LMMB by binding to the corresponding recognition fragment and trigger the isothermal circular strand-displacement polymerization process to generate a positive readout of the amplified signal for detection of the target DNA with the detection limit of 2.5×10^{-10} M

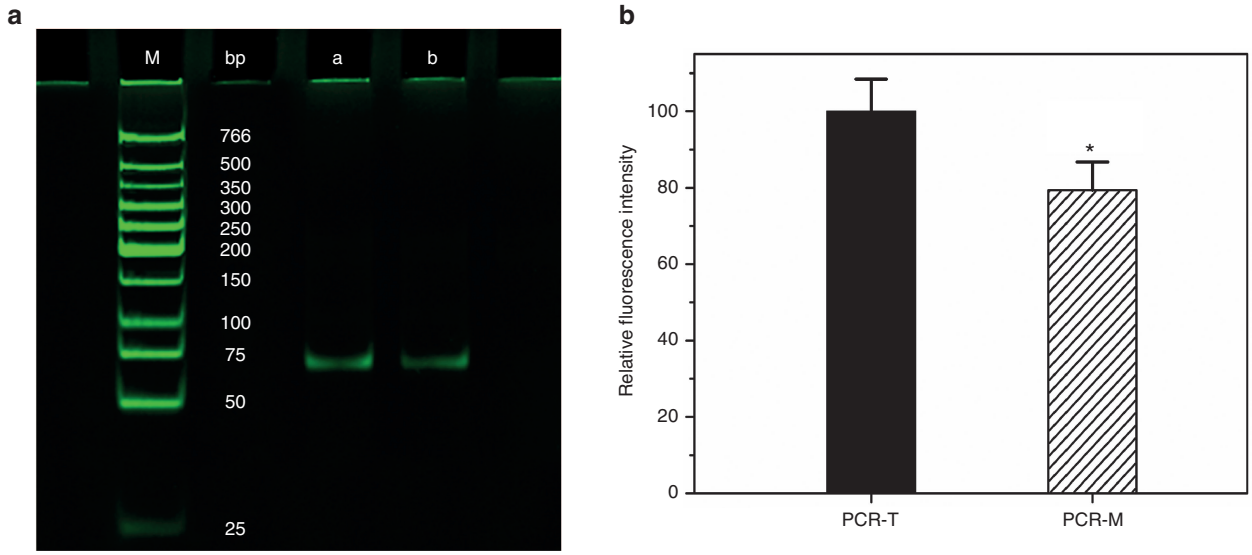

Figure 7 Detection of polymerase chain reaction (PCR) products from real tumor cell lines by label-free multifunctional molecular beacon (LMMB)-based system. (**a**) Image of the 10% native-PAGE gel electrophoresis of the PCR amplicons. Lane M was the DNA markers, while lane a was the PCR product of LOVO cells for wild-type (PCR-T) and lane b was the PCR product of SW 620 cells for mutant-type (PCR-M). (**b**) The relative fluorescence intensity (F_r) of the LMMB-based system for different PCR amplicons (PCR-T and PCR-M). The F_r signal (%) was calculated by the equation: $F_r = (F_m - F_0)/(F_t - F_0) \times 100\%$, where F_t, F_m, and F_0 are the fluorescence intensities in the presence of PCR-T, PCR-M, and blank, respectively. The signal intensity triggered by target DNA is defined as 100%. The error bars are standard deviations of measurements ($n = 3$) of each DNA concentration. The statistical analysis represents the means ± SD of three independent measurements as compared with the control (*$P < 0.05$, **$P < 0.01$).

and dynamic range of 2.0×10^{-9} to 1.0×10^{-7} M without any additional nucleotide sequences and chemical modification. The LMMB could precisely sense a single base mutation.

Materials and methods

Chemicals. All designed oligonucleotides were purchased from Invitrogen Bio (Guangzhou, China), and their sequences were detailed in **Table 1**. The secondary structures of all oligonucleotides were estimated using bioinformatics software (http://mfold.rna.albany.edu/). All oligonucleotides were dissolved in deionized water and stored at 4 °C prior to use. SYBR Green I was purchased from Dingguo Biochemical Reagents Company (Beijing, China), which is 10,000-fold concentrated solution dissolved in dimethyl sulphoxide, while the corresponding working solution was prepared by diluting the stock solution with water. The polymerase Klenow Fragment (Large Fragment *Escherichia coli* DNA Ploymerase I, KF) including the 10× Klenow Fragment buffer and DNA ladder (DL500) were purchased from Takara Biotechnology (Dalian, China). The low molecular weight ladders were purchased from New England Biolabs (Ipswich, MA). The mixture of deoxyribonucleoside 5'-triphosphate (dNTPs) was purchased from Gen-View Scientific (Calimesa, CA). The other chemical reagents were of analytical-reagent grade. Deionized water obtained from a Millipore water purification system (resistance > 18 M·cm, Milli-Q, Millipore) was used throughout the experiments.

Fluorescence measurements. All fluorescence measurements were carried out on a Cary Eclipse fluorescence spectrometer (Varian). Excitation and emission slits were set at 5.0 and 10.0 nm, respectively. The mixture in square quartz cuvettes was excited at 494 nm, and the emission spectra were collected from 500 to 650 nm. The fluorescence intensity at 524 nm was used to evaluate the capability of the proposed probe to screen target DNAs. The experiments were performed at room temperature unless otherwise indicated.

Amplification detection of target DNA. The detection of target *p53* DNA was carried out under identical experimental conditions; and the detection procedure is as follows. At first, a mixture of LMMB (4 µl, 10 µmol/l), 2 µl of the target *p53* DNA at specific concentration, 5 µl of 10× Klenow Fragment buffer and 30.5 µl of deionized water was prepared in a 0.5 ml tube. The mixture was heated to 90 °C for 5 minutes and then cooled to room temperature for 1 hour. Subsequently, 2 µl of 10 mmol/l dNTPs and 0.5 µl of KF polymerase (5 U/µl) were injected into the mixture, and the resulting solution was incubated at 37 °C for 20 minutes with gentle shaking. Finally, 40 µl of 1× Klenow Fragment buffer and 5 µl of SYBR Green I (1,000-fold) were added to make a final volume of reaction solution 100 µl. Fifteen minutes later, the fluorescence spectrum was collected. When evaluating the detection specificity of LMMB-based system, the mutant *p53* DNA was used instead, and the similar procedure was adopted. The fluorescent signals induced by mutant DNAs were determined in comparison with the signals from wild-type *p53* target DNA.

Ligation reaction. The LMMB (2 µl, 10 µmol/l), phosphorylated replication product DNA (PRPD) (2 µl, 10 µmol/l), 10× ligase buffer (5 µl), *E. coli* DNA ligase (0.2 µl, 5 U/µl), and water (40.8 µl) are mixed and incubated at room temperature for 45 minutes. Then, the resulting solution was heated at 90 °C for 5 minutes, followed by incubation at room temperature for 30 minutes. The structure of the ligation products was analyzed by gel electrophoresis.

Gel electrophoresis. The gel electrophoresis was performed on 10% native polyacrylamide gel (native-PAGE) at 80 V for 45 minutes using intercalation dye SYBR Green I in 0.5× TBE buffer (4.5 mmol/l Tris, 4.5 mmol/l boric acid, 0.1 mmol/l EDTA, pH 7.9). The DNA sample (10 µl), 10× loading buffer (2 µl), and 100× SYBR Green (2 µl) were mixed and incubated for 10 minutes in the dark before loading into the well. The resulting gel was excited and imaged using a ChemiDoc XRS+ imaging system with Image Lab analysis software (Bio-Rad).

PCR amplification of genomic DNA extraction from tumor cell lines. PCR amplification was performed using a similar method to the literature we described previously.[50] Briefly, the human colorectal cell lines (LOVO for wild-type *p53* and SW620 for mutant *p53*) were cultured at 37 °C in Ham's F12K liquid medium supplemented with 10% fetal calf serum (FCS). The harvested cells (about10^7) were used to extract genomic DNA using the TaKaRa MiniBEST Universal Genomic DNA Extraction Kit Ver.5.0 (Takara Biotechnology). PCR amplification of *p53* codon 273 was obtained by the following procedure: the reaction solution (genomic DNA, the forward primer 1 and reverse primer 1) as denatured at 90 °C for 5 minutes, followed by 30 cycles at 90 °C for 30 seconds, 55 °C for 45 seconds, 75 °C for 30 seconds, and a final extension at 75 °C for 10 minutes. The detection of these PCR products was carried out using the LMMB.

Supplementary material

Figure S1. The effect of KF concentration on the fluorescence response of the LMMB-based biosensor.
Figure S2. Influence of polymerization time on the fluorescence response of the LMMB-based sensing system.
Figure S3. The estimated secondary structures and relative parameters of LMMB (C-hairpin).
Figure S4. The estimated secondary structures and relative parameters of LMMB (G-hairpin).
Figure S5. The estimated secondary structures and relative parameters of Octamer (seen in **Figure 1**).
Figure S6. The estimated secondary structures and relative parameters of tight dimer (seen in **Figure 1**).
Table S1. Reproducibilityof fluorescence measurementof LMMB-based system in the presence of different concentrations of target *p53* DNA.

Acknowledgments This work was supported by Ministry of Science and Technology of China (2015CB931804), National Natural Science Foundation of China (NSFC) grants (U1505225, 81273548, 21275002, and 81472767) and Independent Research Project of State Key Laboratory of Photocatalysis on Energy and Environment (NO. 2014CO1). This research was supported in part by a Graduate Student Fellowship Award from the American Association of Pharmaceutical Scientists Foundation. The authors have declared that no competing interest exists. There are no potential conflicts of interests.

1. Sidransky, D (1997). Nucleic acid-based methods for the detection of cancer. *Science* **278**: 1054–1059.
2. Levin, BC, Cheng, H and Reeder, DJ (1999). A human mitochondrial DNA standard reference material for quality control in forensic identification, medical diagnosis, and mutation detection. *Genomics* **55**: 135–146.
3. Kruglyak, L and Nickerson, DA (2001). Variation is the spice of life. *Nat Genet* **27**: 234–236.
4. Hirschhorn, JN and Daly, MJ (2005). Genome-wide association studies for common diseases and complex traits. *Nat Rev Genet* **6**: 95–108.
5. Sassolas, A, Leca-Bouvier, BD and Blum, LJ (2008). DNA biosensors and microarrays. *Chem Rev* **108**: 109–139.
6. Li, D, Song, S and Fan, C (2010). Target-responsive structural switching for nucleic acid-based sensors. *Acc Chem Res* **43**: 631–641.
7. Luo, M, Chen, X, Zhou, G, Xiang, X, Chen, L, Ji, X *et al.* (2012). Chemiluminescence biosensors for DNA detection using graphene oxide and a horseradish peroxidase-mimicking DNAzyme. *Chem Commun (Camb)* **48**: 1126–1128.
8. Muller, PA and Vousden, KH (2013). *p53* mutations in cancer. *Nat Cell Biol* **15**: 2–8.
9. Sokol, DL, Zhang, X, Lu, P and Gewirtz, AM (1998). Real time detection of DNA RNA hybridization in living cells. *Proc Natl Acad Sci USA* **95**: 11538–11543.
10. Tang, Z, Wang, K, Tan, W, Ma, C, Li, J, Liu, L *et al.* (2005). Real-time investigation of nucleic acids phosphorylation process using molecular beacons. *Nucleic Acids Res* **33**: e97.
11. Li, Y, Zhou, X and Ye, D (2008). Molecular beacons: an optimal multifunctional biological probe. *Biochem Biophys Res Commun* **373**: 457–461.
12. Wang, K, Tang, Z, Yang, CJ, Kim, Y, Fang, X, Li, W *et al.* (2009). Molecular engineering of DNA: molecular beacons. *Angew Chem Int Ed Engl* **48**: 856–870.
13. Udaya Bhaskara Rao, T and Pradeep, T (2010). Luminescent Ag7 and Ag8 clusters by interfacial synthesis. *Angew Chem Int Ed Engl* **49**: 3925–3929.
14. Petty, JT, Sengupta, B, Story, SP and Degtyareva, NN (2011). DNA sensing by amplifying the number of near-infrared emitting, oligonucleotide-encapsulated silver clusters. *Anal Chem* **83**: 5957–5964.
15. Petty, JT, Story, SP, Juarez, S, Votto, SS, Herbst, AG, Degtyareva, NN *et al.* (2012). Optical sensing by transforming chromophoric silver clusters in DNA nanoreactors. *Anal Chem* **84**: 356–364.
16. Deng, S, Cheng, L, Lei, J, Cheng, Y, Huang, Y and Ju, H (2013). Label-free electrochemiluminescent detection of DNA by hybridization with a molecular beacon to form hemin/G-quadruplex architecture for signal inhibition. *Nanoscale* **5**: 5435–5441.
17. Dong, H, Hao, K, Tian, Y, Jin, S, Lu, H, Zhou, SF *et al.* (2014). Label-free and ultrasensitive microRNA detection based on novel molecular beacon binding readout and target recycling amplification. *Biosens Bioelectron* **53**: 377–383.
18. Heid, CA, Stevens, J, Livak, KJ and Williams, PM (1996). Real time quantitative PCR. *Genome Res* **6**: 986–994.
19. Wang, XL, Li, F, Su, YH, Sun, X, Li, XB, Schluesener, HJ *et al.* (2004). Ultrasensitive detection of protein using an aptamer-based exonuclease protection assay. *Anal Chem* **76**: 5605–5610.
20. Nallur, G, Luo, C, Fang, L, Cooley, S, Dave, V, Lambert, J *et al.* (2001). Signal amplification by rolling circle amplification on DNA microarrays. *Nucleic Acids Res* **29**: E118.
21. Giljohann, DA and Mirkin, CA (2009). Drivers of biodiagnostic development. *Nature* **462**: 461–464.
22. Weizmann, Y, Beissenhirtz, MK, Cheglakov, Z, Nowarski, R, Kotler, M and Willner, I (2006). A virus spotlighted by an autonomous DNA machine. *Angew Chem Int Ed Engl* **45**: 7384–7388.
23. Guo, Q, Yang, X, Wang, K, Tan, W, Li, W, Tang, H *et al.* (2009). Sensitive fluorescence detection of nucleic acids based on isothermal circular strand-displacement polymerization reaction. *Nucleic Acids Res* **37**: e20.
24. Ding, C, Li, X, Ge, Y and Zhang, S (2010). Fluorescence detection of telomerase activity in cancer cells based on isothermal circular strand-displacement polymerization reaction. *Anal Chem* **82**: 2850–2855.
25. Qiu, LP, Wu, ZS, Shen, GL and Yu, RQ (2011). Highly sensitive and selective bifunctional oligonucleotide probe for homogeneous parallel fluorescence detection of protein and nucleotide sequence. *Anal Chem* **83**: 3050–3057.
26. Xuan, F, Luo, X and Hsing, IM (2012). Ultrasensitive solution-phase electrochemical molecular beacon-based DNA detection with signal amplification by exonuclease III-assisted target recycling. *Anal Chem* **84**: 5216–5220.
27. Zhou, H, Xie, SJ, Zhang, SB, Shen, GL, Yu, RQ and Wu, ZS (2013). Isothermal amplification system based on template-dependent extension. *Chem Commun (Camb)* **49**: 2448–2450.
28. Cheng, W, Zhang, W, Yan, Y, Shen, B, Zhu, D, Lei, P *et al.* (2014). A novel electrochemical biosensor for ultrasensitive and specific detection of DNA based on molecular beacon mediated circular strand displacement and rolling circle amplification. *Biosens Bioelectron* **62**: 274–279.
29. Miao, X, Guo, X, Xiao, Z and Ling, L (2014). Electrochemical molecular beacon biosensor for sequence-specific recognition of double-stranded DNA. *Biosens Bioelectron* **59**: 54–57.
30. Xuan, F, Luo, X and Hsing, IM (2012). Sensitive immobilization-free electrochemical DNA sensor based on isothermal circular strand displacement polymerization reaction. *Biosens Bioelectron* **35**: 230–234.
31. Li, Z, Zhu, W, Zhang, J, Jiang, J, Shen, G and Yu, R (2013). A label-free amplified fluorescence DNA detection based on isothermal circular strand-displacement polymerization reaction and graphene oxide. *Analyst* **138**: 3616–3620.

32. Zhang, X, Xu, Y, Zhao, Y and Song, W (2013). A new photoelectrochemical biosensors based on DNA conformational changes and isothermal circular strand-displacement polymerization reaction. *Biosens Bioelectron* **39**: 338–341.
33. Luo, M, Li, N, Liu, Y, Chen, C, Xiang, X, Ji, X *et al.* (2014). Highly sensitive and multiple DNA biosensor based on isothermal strand-displacement polymerase reaction and functionalized magnetic microparticles. *Biosens Bioelectron* **55**: 318–323.
34. Xu, J, Dong, H, Shen, W, He, S, Li, H, Lu, Y *et al.* (2015). New molecular beacon for *p53* gene point mutation and significant potential in serving as the polymerization primer. *Biosens Bioelectron* **66**: 504–511.
35. Feng, K, Qiu, LP, Yang, Y, Wu, ZS, Shen, GL and Yu, RQ (2011). Label-free optical bifunctional oligonucleotide probe for homogeneous amplification detection of disease markers. *Biosens Bioelectron* **29**: 66–75.
36. Zhou, H, Xie, SJ, Li, JS, Wu, ZS and Shen, GL (2012). Intermolecular G-quadruplex-based universal quencher free molecular beacon. *Chem Commun (Camb)* **48**: 10760–10762.
37. Nazarenko, I, Pires, R, Lowe, B, Obaidy, M and Rashtchian, A (2002). Effect of primary and secondary structure of oligodeoxyribonucleotides on the fluorescent properties of conjugated dyes. *Nucleic Acids Res* **30**: 2089–2195.
38. Martinez, K, Estevez, MC, Wu, Y, Phillips, JA, Medley, CD and Tan, W (2009). Locked nucleic acid based beacons for surface interaction studies and biosensor development. *Anal Chem* **81**: 3448–3454.
39. Knemeyer, JP, Marmé, N and Sauer, M (2000). Probes for detection of specific DNA sequences at the single-molecule level. *Anal Chem* **72**: 3717–3724.
40. Stöhr, K, Häfner, B, Nolte, O, Wolfrum, J, Sauer, M and Herten, DP (2005). Species-specific identification of mycobacterial 16S rRNA PCR amplicons using smart probes. *Anal Chem* **77**: 7195–7203.
41. Sauer, M, Han, KT, Müller, R, Nord, S, Schulz, A, Seeger, S *et al.* (1995). New fluorescent dyes in the red region for biodiagnostics. *J Fluoresc* **5**: 247–261.
42. Lieberwirth, U, Arden-Jacob, J, Drexhage, KH, Herten, DP, Müller, R, Neumann, M *et al.* (1998). Multiplex dye DNA sequencing in capillary gel electrophoresis by diode laser-based time-resolved fluorescence detection. *Anal Chem* **70**: 4771–4779.
43. Shlyahovsky, B, Li, D, Weizmann, Y, Nowarski, R, Kotler, M and Willner, I (2007). Spotlighting of cocaine by an autonomous aptamer-based machine. *J Am Chem Soc* **129**: 3814–3815.
44. Xiao, Y, Pavlov, V, Niazov, T, Dishon, A, Kotler, M and Willner, I (2004). Catalytic beacons for the detection of DNA and telomerase activity. *J Am Chem Soc* **126**: 7430–7431.
45. Liu, X and Tan, W (1999). A fiber-optic evanescent wave DNA biosensor based on novel molecular beacons. *Anal Chem* **71**: 5054–5059.
46. Wu, ZS, Zhang, S, Zhou, H, Shen, GL and Yu, R (2010). Universal aptameric system for highly sensitive detection of protein based on structure-switching-triggered rolling circle amplification. *Anal Chem* **82**: 2221–2227.
47. Wu, ZS, Zhou, H, Zhang, S, Shen, G and Yu, R (2010). Electrochemical aptameric recognition system for a sensitive protein assay based on specific target binding-induced rolling circle amplification. *Anal Chem* **82**: 2282–2289.
48. Huang, CC, Huang, YF, Cao, Z, Tan, W and Chang, HT (2005). Aptamer-modified gold nanoparticles for colorimetric determination of platelet-derived growth factors and their receptors. *Anal Chem* **77**: 5735–5741.
49. Yang, L, Fung, CW, Cho, EJ and Ellington, AD (2007). Real-time rolling circle amplification for protein detection. *Anal Chem* **79**: 3320–3329.
50. Qiu, LP, Chen, L and Chen, KP (2014). Antihepatitis B therapy: a review of current medications and novel small molecule inhibitors. *Fundam Clin Pharmacol* **28**: 364–381.

Supplementary Information accompanies this paper on the Molecular Therapy–Nucleic Acids website (http://www.nature.com/mtna)